Modelling and Simulation of a Quantum Wire to Study the Coexistence of Rashba and Dresselhaus Spin-Orbit Couplings

Xi FU*[1,2] , Yuanping CHEN[2], Haixia GAO[1]

[1.] College of Science, Hunan University of Science and Engineering, Yongzhou, Hunan 425199, China;
[2.] *School of Physics and Optoelectronics*, XiangTan University, Xiangtan, Hunan 411105, China

***Abstract* — We investigate the spin accumulation of a quantum wire (QW) nonadiabatically connected to two leads with the coexistence of Rashba and Dresselhaus spin-orbit coupling (SOC) in the wire and two leads respectively. Using scattering matrix approach and perturbation theory, three components of spin polarization S_i (i=x,y,z) for the system have been calculated. When no SOC present in two leads, the RSOC in the QW leads to the formation of out-of-plane spin accumulation while no spin accumulation indicates for the DOC case in the QW, as well as when two SOC terms coexist in the QW the influences of RSOC are dominant to the spin accumulation and its symmetry is broken due to the existence of DSOC. Moreover we find out for two SOCs in the QW case the spin precession length is $L_{SOC} = \frac{\hbar^2}{2m^*}\sqrt{\alpha_R^2 + \beta_D^2}$, and longitudinal oscillations of spin polarization can be used to differentiate intrinsic spin accumulation from the extrinsic one by changing two SOC strengths. Furthermore, when there have SOCs in the QW and two leads, the RSOC in two leads enhances the strength of spin polarization while the DSOC in two leads decrease it, moreover, the out-of-plane spin accumulation still present and two SOC terms in the leads shift intrinsic oscillations of in-plane spin polarizations and change the strength of spin accumulation accordingly, which means that one can also realize the manipulation of spin polarization and spin accumulation by altering the SOC terms in two leads.**

Keywords - Quantum wire; Spin-orbit coupling; Spin accumulation

I. INTRODUCTION

The presence of electronic spin degree of freedom in nanoscale and mesoscale semiconductor systems has driven a large amount of research during the past decades. Prominent examples range from spintronics[1,2], over spin qubits [3] to topological insulators [4], and the quantum spin Hall effect [5,6].

One important effect is thereby the coupling between the electron spin and its motion which provides us with a new freedom to control the electron spin via electric field [7]. There are two types of intrinsic SOC in semiconductor two-dimensional electron gas (2DEG). One is Rashba SOC (RSOC) produced by the inversion asymmetry structure of potential confining 2DEG, which is extensively studied for its strength can be controlled by gate voltage (electric field) [8]. The other is Dresselhaus SOC (DSOC) induced by the bulk inversion asymmetry of zinc-blende type crystal structure [9]. In some 2DEG systems, the DSOC can lead to linear k-splitting and its strength increases with the decreasing of thickness [10], therefore, the DSOC would be comparable with the RSOC [11]. Both RSOC and DSOC can result in spin splitting of bands and give rise to a variety of spin-dependent phenomena.

Spin-dependent transports in two-dimensional structures with two intrinsic SOCs (the RSOC and the DSOC) have been intensively studied [12-23] and the interplay between the two SOCs leads to significant changes in the transport properties. Schliemann *et al.* [13] proposed a nonballistic spin-field-effect transistor based on the competition between RSOC and DSOC. The anisotropic spin transport with two SOC terms in two-terminal mesoscopic rings and GaAs quantum wells has been studied, respectively [14,15], where the initial symmetry is broken. Experimentally, Giglberger *et al.* [16,17] pointed out that the ratio of relevant Rashba and Dresselhaus coefficients can be deduced directly from experiments using the spin-galvanic effect, and further Scheid *et al.* [18] proposed a new method to determine relative strength of Rashba and Dresselhaus spin-orbit interaction by numerical calculations of the conductance of quantum wires (QWs) based on the Landauer formalism. For the spin accumulation, Yao and Yang [19] and Wang *et al.* [20] have studied the symmetry properties of spin accumulation in a Rashba bar and the intrinsic oscillations of accumulation in a Rashba QW, respectively. When the RSOC and the DSOC coexists, Chen *et al.* [21] have studied the out-of-plane spin accumulation in a four-terminal setup using the real space Landauer-Keldysh formalism, and the spin-Hall accumulation symmetry is broken by magnetic field or coexistence of two SOC terms. Pandey [22] studied spin accumulation due to double refraction at lithographic boundaries, as well as the interplay between Rashba and Dresselhaus spin-orbit coupling gives rise to anisotropy in Fermi energy surface and a non-zero net spin-polarized current and spin accumulation at the edges are observed.

In the present paper we study spin polarization and spin accumulation of a QW which is attached to two leads with the coexistence of RSOC and DSOC in the wire and two leads respectively (see Fig.1) by using the scattering matrix

approach. The influences of Rashba and Dresselhaus strength on three components of spin polarization for the system have been studied and discussed.

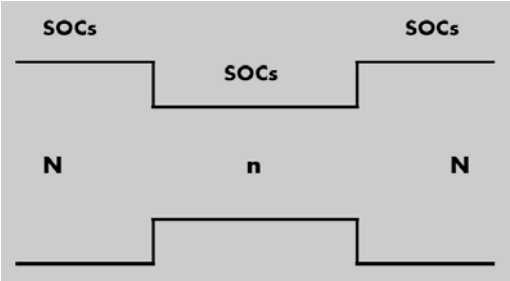

Figure 1. The geometry of QW system in which the RSOC and the DSOC coexist in the QW (propagation modes n) and two leads (propagation modes N), respectively.

II. MODE AND FORMALISM

We start with the effective mass single-electron Hamiltonian for the QW and two leads

$$H_{QW} = H_0 + H_R + H_D,\ H_{lead} = H_0 + H_{RN} + H_{DN} \tag{1}$$

where

$$H_0 = -\frac{\hbar^2}{2m^*}(\frac{\partial^2}{\partial x^2} + \frac{\partial^2}{\partial y^2}) + V(x) \tag{2}$$

is the uncoupled Hamiltonian and

$$H_R = i\alpha_R(\sigma_x \frac{\partial}{\partial y} - \sigma_y \frac{\partial}{\partial x}),\ H_{RN} = i\alpha_{RN}(\sigma_x \frac{\partial}{\partial y} - \sigma_y \frac{\partial}{\partial x}) \tag{3}$$

$$H_D = i\beta_D(\sigma_x \frac{\partial}{\partial x} - \sigma_y \frac{\partial}{\partial y}),\ H_{DN} = i\beta_{DN}(\sigma_x \frac{\partial}{\partial x} - \sigma_y \frac{\partial}{\partial y}) \tag{4}$$

the RSOC and the DSOC Hamiltonian [14,15] for the QW and two leads. In the above Hamiltonians, the lateral confining potential [14] V(x)=0 for |x|<d/2 (or |x|<D/2) and $=\infty$ for |x|>d/2 (or |x|>D/2) with d (D) the width of QW (Leads), while α_R (α_{RN}) and β_D (β_{DN}) denote Rashba and Dresselhaus strength for the QW and two leads respectively. m^* and $\sigma_{x/y}$ are the effective electron mass and *x/y*-component of pauli matrix.

We assume that an electron wave is injected from the left lead with two SOC terms into the QW also with the two terms. Due to the translational invariance in the longitudinal y-direction in Hamiltonlian (1), the wave functions respectively for spin-up ($\uparrow$) and -down ($\downarrow$) electrons in the QW and two leads are the multiplication of a plane wave and a transversally confined wave function respectively. In the case of weak SOC, the corresponding transverse wave functions $\varphi_{n\uparrow\downarrow}$ for the QW and $\phi_{N\uparrow\downarrow}$ for the leads can be analytically solved by perturbation as [23]

$$\varphi_{n\uparrow\downarrow} = \sqrt{\frac{2}{d}}\sin[\frac{n\pi}{d}(x+\frac{d}{2})] \pm \sum_{m\neq n} A_{mn}\sin[\frac{m\pi}{d}(x+\frac{d}{2})] + i\sum_{m\neq n} B_{mn}\sin[\frac{m\pi}{d}(x+\frac{d}{2})] \tag{5}$$

$$\phi_{n\uparrow\downarrow} = \sqrt{\frac{2}{D}}\sin[\frac{N\pi}{D}(x+\frac{D}{2})] \pm \sum_{M\neq N} A_{MN}\sin[\frac{M\pi}{D}(x+\frac{D}{2})] + i\sum_{M\neq N} B_{MN}\sin[\frac{M\pi}{D}(x+\frac{D}{2})] \tag{6}$$

where

$$A_{mn} = \frac{4mn[1-(-1)^{m+n}]}{m^2-n^2}\frac{m^* d\alpha_R}{\pi^2\hbar^2},$$

$$B_{mn} = \frac{4mn[1-(-1)^{m+n}]}{m^2-n^2}\frac{m^* d\beta_D}{\pi^2\hbar^2}(m,n=0,1,2,\ldots), \tag{7}$$

$$A_{MN} = \frac{4MN[1-(-1)^{M+N}]}{M^2-N^2}\frac{m^* D\alpha_{RN}}{\pi^2\hbar^2},$$

$$B_{MN} = \frac{4MN[1-(-1)^{M+N}]}{M^2-N^2}\frac{m^* D\beta_{DN}}{\pi^2\hbar^2}(M,N=0,1,2,\ldots). \tag{8}$$

The corresponding electron energies in the QW are $E_{\uparrow\downarrow} = \frac{\hbar^2 k_{n\uparrow\downarrow}^2}{2m^*} + \varepsilon_{n\uparrow\downarrow}$ with the lateral sublevels

$$\varepsilon_{n\uparrow} = \frac{n^2\hbar^2\pi^2}{2m^* d} + \sqrt{\alpha_R^2+\beta_D^2}k_{n\uparrow} \text{ and } \varepsilon_{n\downarrow} = \frac{n^2\hbar^2\pi^2}{2m^* d} - \sqrt{\alpha_R^2+\beta_D^2}k_{n\downarrow},$$

and the corresponding electron energies in two leads are $E_{\uparrow\downarrow} = \frac{\hbar^2 k_{N\uparrow\downarrow}^2}{2m^*} + \varepsilon_{N\uparrow\downarrow}$ with the lateral sublevels $\varepsilon_{N\uparrow} = \frac{N^2\hbar^2\pi^2}{2m^* D} + \sqrt{\alpha_{RN}^2+\beta_{DN}^2}k_{N\uparrow}$ and $\varepsilon_{N\downarrow} = \frac{N^2\hbar^2\pi^2}{2m^* D} - \sqrt{\alpha_{RN}^2+\beta_{DN}^2}k_{N\downarrow}$.

Therefore, the longitudinal wavevectors can be expressed as

$$k_{n\uparrow}^{\pm}(E_\uparrow) = \frac{m^*}{\hbar^2}[-\sqrt{\alpha_R^2+\beta_D^2} \pm \sqrt{\alpha_R^2+\beta_D^2+2\hbar^2(E_\uparrow - n^2\hbar^2\pi^2/(2m^* d))/m^*}], \tag{9}$$

$$k_{n\downarrow}^{\pm}(E_\downarrow) = \frac{m^*}{\hbar^2}[\sqrt{\alpha_R^2+\beta_D^2} \pm \sqrt{\alpha_R^2+\beta_D^2+2\hbar^2(E_\downarrow - n^2\hbar^2\pi^2/(2m^* d))/m^*}] \tag{10}$$

and

$$k_{N\uparrow}^{\pm}(E_\uparrow) = \frac{m^*}{\hbar^2}[-\sqrt{\alpha_{RN}^2+\beta_{DN}^2} \pm \sqrt{\alpha_{RN}^2+\beta_{DN}^2+2\hbar^2(E_\uparrow - N^2\hbar^2\pi^2/(2m^* D))/m^*}], \tag{11}$$

$$k^{\pm}_{N\downarrow}(E_\downarrow)=\frac{m^*}{\hbar^2}[\sqrt{\alpha^2_{RN}+\beta^2_{DN}}\pm \sqrt{\alpha^2_{RN}+\beta^2_{DN}+2\hbar^2(E_\downarrow-N^2\hbar^2\pi^2/(2m^*D))/m^*}] \quad (12)$$

for spin-up and -down electrons, respectively.

In order to calculate the scattering matrices separately for spin-up and -down electrons, one needs to match the wave functions at two interfaces of wire-lead connection. However, for a symmetric system one can calculate the scattering matrices for one interface as if without other interface, and the total scattering matrices can be obtained by the symmetry property of QW system [24]. Therefore, we first calculate the left interface (y=0), then in the left lead the wave functions for spin-up and -down electrons can be written as

$$\psi_\uparrow(x,y<0)=\phi_{N\uparrow}(x)e^{iK^+_{N\uparrow}y}+\sum_{N'}r_{N'\uparrow N}\phi_{N'\uparrow}(x)e^{-iK^+_{N'\uparrow}y}, \quad (13)$$

$$\psi_\downarrow(x,y<0)=\phi_{N\downarrow}(x)e^{iK^+_{N\downarrow}y}+\sum_{N'}r_{N'\downarrow N}\phi_{N'\downarrow}(x)e^{-iK^+_{N'\downarrow}y}, \quad (14)$$

where $r_{N'\uparrow N}$ ($r_{N'\downarrow N}$) is the coefficient of incident modes N (including $N_\uparrow$ and $N_\downarrow$) reflecting to mode $N'_\uparrow$ ($N'_\downarrow$) respectively. In the QW the wave functions for spin-up and -down electrons are

$$\psi_\uparrow(x,y\geq 0)=\sum_{n'}t'_{n'\uparrow N}\varphi_{n'\uparrow}(x)e^{ik^+_{n'\uparrow}y}, \quad (15)$$

$$\psi_\downarrow(x,y\geq 0)=\sum_{n'}t'_{n'\downarrow N}\varphi_{n'\downarrow}(x)e^{ik^+_{n'\downarrow}y}, \quad (16)$$

where $t'_{n'\uparrow N}$ ($t'_{n'\downarrow N}$) is coefficient of incident modes N transmitting to mode $n_\uparrow$ ($n_\downarrow$).

The continuity of the wave functions at left interface y=0 gives

$$\phi_{N\uparrow}(x)+\sum_{N'}r_{N'\uparrow N}\phi_{N'\uparrow}(x)=\sum_{n'}t'_{n'\uparrow N}\varphi_{n'\uparrow}(x)$$
$$\phi_{N\downarrow}(x)+\sum_{N'}r_{N'\downarrow N}\phi_{N'\downarrow}(x)=\sum_{n'}t'_{n'\downarrow N}\varphi_{n'\downarrow}(x). \quad (17)$$

The continuity of the derivative of wave functions may not hold due to the existence of two SOC terms. However, the current conservation for the system still holds [23,25]

$$\begin{bmatrix} -i\frac{\hbar}{m^*}\frac{\partial}{\partial y} & \frac{\alpha_{RN}-i\beta_{DN}}{\hbar} \\ \frac{\alpha_{RN}+i\beta_{DN}}{\hbar} & -i\frac{\hbar}{m^*}\frac{\partial}{\partial y}\end{bmatrix}\begin{bmatrix}\psi_\uparrow(x,y<0)\\ \psi_\downarrow(x,y<0)\end{bmatrix}=$$
$$\begin{bmatrix} -i\frac{\hbar}{m^*}\frac{\partial}{\partial y} & \frac{\alpha_R-i\beta_D}{\hbar} \\ \frac{\alpha_R+i\beta_D}{\hbar} & -i\frac{\hbar}{m^*}\frac{\partial}{\partial y}\end{bmatrix}\begin{bmatrix}\psi_\uparrow(x,y\geq 0)\\ \psi_\downarrow(x,y\geq 0)\end{bmatrix}, \quad (18)$$

hence one can obtain

$$K^+_{N\uparrow}\phi_{N\uparrow}(x)-\sum_{N'}r_{N'\uparrow N}K^+_{N'\uparrow}\phi_{N'\uparrow}(x)+\frac{(\alpha_{RN}-i\beta_{DN})m^*}{\hbar^2}[\phi_{N\downarrow}(x)+\sum_{N'}r_{N'\downarrow N}\phi_{N'\downarrow}(x)]=\sum_{n'}t'_{n'\uparrow N}k^+_{n'\uparrow}\varphi_{n'\uparrow}(x)+\sum_{n'}\frac{(\alpha_R-i\beta_D)m^*}{\hbar^2}t'_{n'\downarrow N}\varphi_{n'\downarrow}(x),$$

$$K^+_{N\downarrow}\phi_{N\downarrow}(x)-\sum_{N'}r_{N'\downarrow N}K^+_{N'\downarrow}\phi_{N'\downarrow}(x)+\frac{(\alpha_{RN}+i\beta_{DN})m^*}{\hbar^2}[\phi_{N\uparrow}(x)+\sum_{N'}r_{N'\uparrow N}\phi_{N'\uparrow}(x)]=\sum_{n'}t'_{n'\downarrow N}k^+_{n'\downarrow}\varphi_{n'\downarrow}(x)+\sum_{n'}\frac{(\alpha_R+i\beta_D)m^*}{\hbar^2}t'_{n'\uparrow N}\varphi_{n'\uparrow}(x). \quad (19)$$

Multiplying $\phi_{N\uparrow\downarrow}(x)$ and $\varphi_{n\uparrow\downarrow}(x)$ with Eqs.(17) and (19), respectively, and integrating over the range of -d/2<x<d/2, one obtains the matrices of reflection $r_{\uparrow\downarrow}$ and transmission $t'_{\uparrow\downarrow}$ at the y=0 interface as

$$r_\uparrow=Q^{-1}_\uparrow(\lambda_\uparrow t'_\uparrow-1),\quad r_\downarrow=Q^{-1}_\downarrow(\lambda_\downarrow t'_\downarrow-1) \quad (20)$$

and

$$t'_\uparrow=[Ab-Bb*Aa^{-1}*Ba]^{-1}\times[Db-Bb*Aa^{-1}*Da],$$
$$t'_\downarrow=[Aa-Ba*Ab^{-1}*Bb]^{-1}\times[Da-Ba*Ab^{-1}*Db] \quad (21)$$

with

$$Aa=\chi_\uparrow-\gamma^T_\uparrow Q^{-1}_\downarrow\lambda_\downarrow,\quad Ab=\chi_\downarrow-\gamma^T_\downarrow Q^{-1}_\uparrow\lambda_\uparrow, \quad (22)$$

$$Ba=\lambda^T_\uparrow K_{N\uparrow}Q^{-1}_\uparrow\lambda_\uparrow+k_{n\uparrow}q_\uparrow,$$

$$Bb=\lambda^T_\downarrow K_{N\downarrow}Q^{-1}_\downarrow\lambda_\downarrow+k_{n\downarrow}q_\downarrow, \quad (23)$$

$$Da=\lambda^T_\uparrow(1+Q^{-1}_\uparrow)K_{N\uparrow}+\gamma^T_\uparrow(1-Q^{-1}_\downarrow),$$

$$Db=\lambda^T_\downarrow(1+Q^{-1}_\downarrow)K_{N\downarrow}+\gamma^T_\downarrow(1-Q^{-1}_\uparrow), \quad (24)$$

where the corresponding matrix elements are

$$Q_\uparrow=Q_{N\uparrow N'\uparrow}=\int^{d/2}_{-d/2}\phi_{N\uparrow}(x)\phi_{N'\uparrow}(x)dx,$$

$$Q_\downarrow=Q_{N\downarrow N'\downarrow}=\int^{d/2}_{-d/2}\phi_{N\downarrow}(x)\phi_{N'\downarrow}(x)dx,$$

$$q_{\uparrow} = q_{n\uparrow n'\uparrow} = \int_{-d/2}^{d/2} \varphi_{n\uparrow}(x)\varphi_{n'\uparrow}(x)dx,$$

$$q_{\downarrow} = q_{n\downarrow n'\downarrow} = \int_{-d/2}^{d/2} \varphi_{n\downarrow}(x)\varphi_{n'\downarrow}(x)dx,$$

$$p_{\uparrow} = p_{n\uparrow n\downarrow} = \frac{(\alpha_R - i\beta_D)m^*}{\hbar^2}\int_{-d/2}^{d/2} \varphi_{n\uparrow}(x)\varphi_{n\downarrow}(x)dx,$$

$$p_{\uparrow\downarrow} = p_{n\downarrow n\uparrow} = \frac{(\alpha_R + i\beta_D)m^*}{\hbar^2}\int_{-d/2}^{d/2} \varphi_{n\downarrow}(x)\varphi_{n\uparrow}(x)dx,$$

$$\lambda_{\uparrow} = \lambda_{N\uparrow n\uparrow} = \int_{-d/2}^{d/2} \phi_{N\uparrow}(x)\varphi_{n\uparrow}(x)dx,$$

$$\lambda_{\downarrow} = \lambda_{N\downarrow n\downarrow} = \int_{-d/2}^{d/2} \phi_{N\downarrow}(x)\varphi_{n\downarrow}(x)dx,$$

$$\chi_{\uparrow} = \chi_{n\uparrow n'\downarrow} = \frac{(\alpha_R - i\beta_D)m^*}{\hbar^2}\int_{-d/2}^{d/2} \varphi_{n\uparrow}(x)\varphi_{n'\downarrow}(x)dx,$$

$$\chi_{\downarrow} = \chi_{n\downarrow n'\uparrow} = \frac{(\alpha_R + i\beta_D)m^*}{\hbar^2}\int_{-d/2}^{d/2} \varphi_{n\downarrow}(x)\varphi_{n'\uparrow}(x)dx,$$

$$\gamma_{\uparrow} = \gamma_{N\downarrow n\uparrow} = \frac{(\alpha_{RN} - i\beta_{DN})m^*}{\hbar^2}\int_{-d/2}^{d/2} \phi_{N\downarrow}(x)\varphi_{n\uparrow}(x)dx,$$

$$\gamma_{\downarrow} = \gamma_{N\uparrow n\downarrow} = \frac{(\alpha_{RN} + i\beta_{DN})m^*}{\hbar^2}\int_{-d/2}^{d/2} \phi_{N\uparrow}(x)\varphi_{n\downarrow}(x)dx,$$

$$K_{N\uparrow\downarrow} = \delta_{NN'}K^{+}_{N\uparrow\downarrow},\ k_{n\uparrow\downarrow} = \delta_{nn'}k^{+}_{n\uparrow\downarrow}. \quad (25)$$

Furthermore, an analogous calculation for an incident wave from right side to left at y=0 interface gives $r'_{\uparrow\downarrow}$ and $t_{\uparrow\downarrow}$ as

$$t_{\uparrow} = Q^{-1}_{\uparrow}\lambda_{\uparrow}(1 + r'_{\uparrow}),\ t_{\downarrow} = Q^{-1}_{\downarrow}\lambda_{\downarrow}(1 + r'_{\downarrow}) \quad (26)$$

and

$$r'_{\uparrow} = [Ab - Bb * Aa^{-1} * Ba]^{-1} \times [Cb - Bb * Aa^{-1} * Ca],$$

$$r'_{\downarrow} = [Aa - Ba * Ab^{-1} * Bb]^{-1} \times [Ca - Ba * Ab^{-1} * Cb] \quad (27)$$

with

$$Ca = -\lambda^{T}_{\uparrow}K_{N\uparrow}Q^{-1}_{\uparrow}\lambda_{\uparrow} + \gamma^{T}_{\uparrow}Q^{-1}_{\downarrow}\lambda_{\downarrow} + k_{n\uparrow} - p_{\uparrow},$$

$$Cb = -\lambda^{T}_{\downarrow}K_{N\downarrow}Q^{-1}_{\downarrow}\lambda_{\downarrow} + \gamma^{T}_{\downarrow}Q^{-1}_{\uparrow}\lambda_{\uparrow} + k_{n\downarrow} - p_{\downarrow}. \quad (28)$$

Therefore, the scattering matrices $S^{(1)}_{\uparrow\downarrow}$ at y=0 interface can be constructed as

$$S^{(1)}_{\uparrow} = \begin{bmatrix} \bar{r}_{N'\uparrow N} & \bar{t}_{N\uparrow n} \\ \bar{t}'_{n\uparrow N} & \bar{r}'_{n'\uparrow n} \end{bmatrix},\ S^{(1)}_{\downarrow} = \begin{bmatrix} \bar{r}_{N'\downarrow N} & \bar{t}_{N\downarrow n} \\ \bar{t}'_{n\downarrow N} & \bar{r}'_{n'\downarrow n} \end{bmatrix}, \quad (29)$$

where the wave amplitudes have been normalized $\bar{t}'_{n\uparrow\downarrow N} = (k^{+}_{n\uparrow\downarrow}/K^{+}_{N\uparrow\downarrow})^{1/2}t'_{n\uparrow\downarrow N}$, $\bar{t}_{N\uparrow\downarrow n} = (K^{+}_{N\uparrow\downarrow}/k^{+}_{n\uparrow\downarrow})^{1/2}t_{N\uparrow\downarrow n}$, $\bar{r}_{N'\uparrow\downarrow N} = (K^{-}_{N'\uparrow\downarrow}/K^{+}_{N\uparrow\downarrow})^{1/2}r_{N'\uparrow\downarrow N}$ and $\bar{r}'_{n'\uparrow\downarrow n} = (k^{-}_{n'\uparrow\downarrow}/k^{+}_{n\uparrow\downarrow})^{1/2}r'_{n'\uparrow\downarrow n}$. Due to the symmetry of QW system, the scattering matrices $S^{(2)}_{\uparrow\downarrow}$ at y=L interface are

$$S^{(2)}_{\uparrow} = \begin{bmatrix} \bar{r}'_{n'\uparrow n} & \bar{t}'_{n\uparrow N} \\ \bar{t}_{N\uparrow n} & \bar{r}_{N'\uparrow N} \end{bmatrix},\ S^{(2)}_{\downarrow} = \begin{bmatrix} \bar{r}'_{n'\downarrow n} & \bar{t}'_{n\downarrow N} \\ \bar{t}_{N\downarrow n} & \bar{r}_{N'\downarrow N} \end{bmatrix}. \quad (30)$$

When the bias V applied to two leads is small, the total spin polarization can be expressed as [19]

$$\langle S_i(x,y)\rangle = \frac{\int_{E_f - eV/2}^{E_f + eV/2} g(E,T)\langle S_i(x,y)\rangle_E dE}{\frac{\hbar}{2}|C|^2\int_{E_f - eV/2}^{E_f + eV/2} g(E,T)dE} \approx \frac{\langle S_i(x,y)\rangle_{E_f}}{\frac{\hbar}{2}|C|^2}, \quad (31)$$

where $\langle S_i(x,y)\rangle_E = \frac{\hbar}{2}\Psi^{+}(x,y,E)\sigma_i\Psi(x,y,E)$ and C is the normalization coefficient. $\Psi(x,y,E)$ is the total electron wave function in the QW and it can be constructed as

$$\Psi(x,y) = \begin{pmatrix} \psi_{\uparrow}(x,y) \\ \psi_{\downarrow}(x,y) \end{pmatrix} = \sum_n \begin{pmatrix} \bar{t}'_{n\uparrow N}\, e^{ik^{+}_{n\uparrow}y}\varphi_{n\uparrow}(x) + \bar{r}'_{n'\uparrow n}\, e^{ik^{+}_{n\uparrow}(L-y)}\varphi_{n\uparrow}(x) \\ \bar{t}'_{n\downarrow N}\, e^{ik^{+}_{n\downarrow}y}\varphi_{n\downarrow}(x) + \bar{r}'_{n'\downarrow n}\, e^{ik^{+}_{n\downarrow}(L-y)}\varphi_{n\downarrow}(x) \end{pmatrix}, \quad (32)$$

$g(E,T) = 1/\{1 + \exp[(E - E_f)/k_BT]\}$ is the equilibrium Fermi distribution function and for the low temperature case $k_BT << E_F$ one can take $E \approx E_F$.

III. RESULTS AND DISCUSSION

In the following we present some numerical examples of calculated spin polarization $\langle S_i(x,y)\rangle (i = x,y,z)$ for the QW system. The electron effective mass [26] is taken as that for InGaAs quantum well m^*=0.04 m_e and the width of leads D=230 nm in which supporting five propagation modes (N=5) at the Fermi energy. The relative transverse position is u=x/d and the QW length L=1200 nm. Moreover for the weak SOC case, the RSOC and the DSOC strength [27] are taken as about ~10^{-11} eVm and the incident electron energy E=E_F=5.9 meV. We first focus on spin polarizations for the case of no SOC terms in two leads, that is, $\alpha_{RN} = \beta_{DN} = 0$ in Fig.2-Fig.5, further spin polarizations for the existence of two SOC terms in two leads have been discussed in Fig.6 and Fig.7.

Figure 2 shows three components of spin polarization S_i (i=x,y,z) for the case of two (Fig.2(a)-Fig.2(c)), four (Fig.2(d)-Fig.2(f)) and six (Fig.2(g)-Fig.2(i)) propagation modes in the QW respectively, and due to N=5 these figures include Wide-Narrow-Wide and Narrow-Wide-Narrow cases. One can find that the out-of-plane spin polarization S_z reveals transverse spin accumulation patterns, that is, when

the number of propagation modes n in the QW increases, along the transverse u direction three components show more oscillations, and two inverse accumulation peaks of S_z shift towards two edges of QW which forms the out-of-plane spin accumulation. [19] Moreover, three components S_i also show oscillations along the longitudinal direction, and with the number of propagation modes increasing the oscillations of in-plane spin polarizations S_x and S_y have been shift due to the coupling of modes.

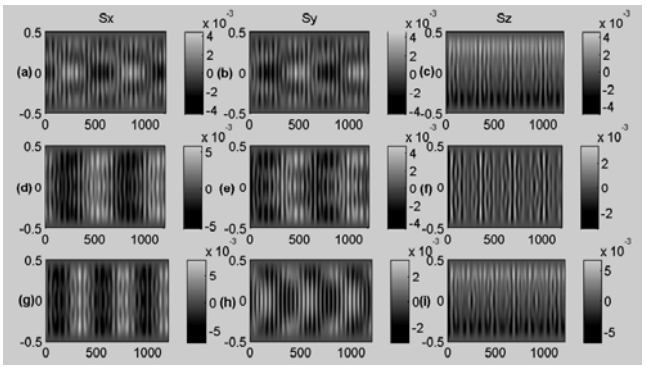

Figure 2. The spin polarization S_i (i=x,y,z) for different number of propagation modes n with α_R =1.0×10^{-11} eVm, β_D =0.5×10^{-11} eVm and $\alpha_{RN}=\beta_{DN}=0$. (a)-(c) for n=2, (d)-(f) for n=4 and (g)-(i) for n=6.

Figure 3-5 show three components of spin polarization S_i (i=x, y, z) for different SOC cases, and present how the RSOC, the DSOC and the ratio of two SOC terms influence the spin polarizations of system when no SOC terms present in two leads.

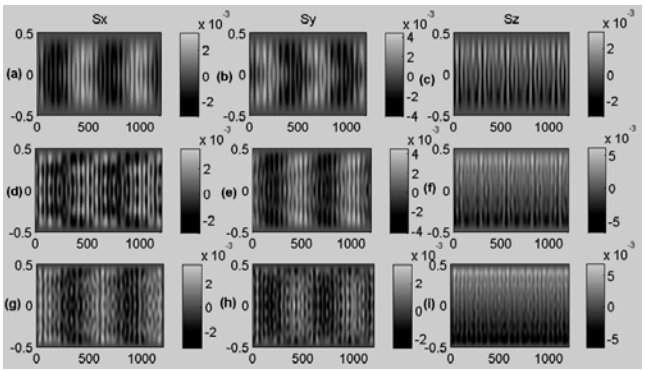

Figure 3. The spin polarization S_i (i=x,y,z) for the case of RSOC with α_R =1.0×10^{-11} eVm (a-b), DSOC with β_D =1.0×10^{-11} eVm (d-f), and two SOC terms with α_R =1.0×10^{-11} eVm and β_D =1.0×10^{-11} eVm (g-i) respectively. The propagation modes n=3 and $\alpha_{RN}=\beta_{DN}=0$.

In Fig.3, three components of spin polarization for the RSOC, the DSOC and two SOC terms cases in the QW have been indicated. From the figures, the in-plane spin polarizations S_x and S_y take on oscillations along the longitudinal direction and the oscillations have been shift by the strength of SOC terms. When two SOC terms coexist, the period of oscillations decreased accordingly indicating that the oscillations of polarization is intrinsic. For the out of plane spin polarization S_z, when only the RSOC exists in Fig.3(c) it presents two inverse and symmetrical spin polarization peaks and out-of-plane spin accumulation forms along u direction. While in Fig.3(f) when only the DSOC exists, no out-of-plane spin accumulation forms. Further, when two SOC terms coexist and take the same strength in Fig.3(i), S_z shows two inverse accumulation peaks and the out-of-plane spin accumulation still possesses indicating that the RSOC is dominated to the out of plane spin polarization. Moreover, due to the spin precession along the longitudinal position of QW system, the period of longitudinal oscillations for α_R =1.0×10^{-11} eVm and β_D=1.0×10^{-11} eVm are equal in length. One notes that the Rashba or Dresselhuas spin precession lengths are 300 nm, which exactly are consistent with the results ($L_{SOC}=\pi\hbar^2/2m^*\alpha_R=\pi\hbar^2/2m^*\beta_D$) in Ref.19 and Ref.28 [19,28], and the presented results may be observable experimentally to differentiate the intrinsic and extrinsic spin accumulation. When two SOC terms coexist, the spin precession length decreases to about 200 nm which means that the precession length should be $L_{SOC}=\pi\hbar^2/(2m^*\sqrt{\alpha_R^2+\beta_D^2})$.

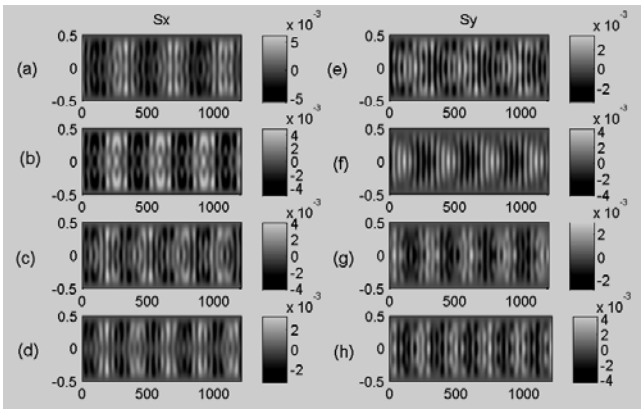

Figure 4. The in-plane spin polarizations S_x and S_y for different strength of two SOC terms cases. (a)-(d) for S_x and (e)-(h) for S_y corresponding to α_R =0.5, 1.0, 1.5, 2.0×10^{-11} eVm with fixed β_D =1.5×10^{-11} eVm, respectively.

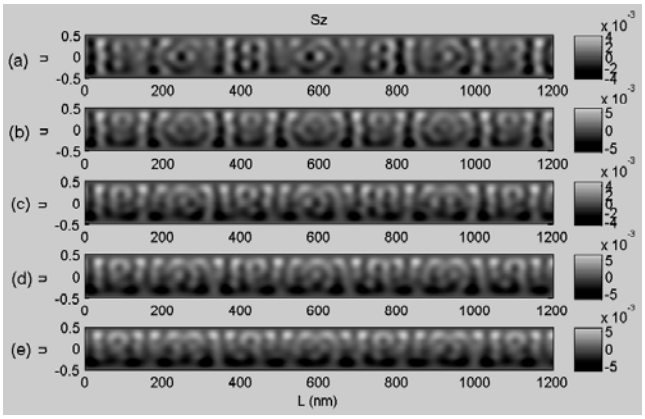

Figure 5. The out of plane spin polarization S_z for different strength of two SOC terms cases. (a)-(e) corresponding to α_R =0.5, 1.0, 1.5, 2.0, 2.5×10^{-11} eVm with fixed β_D =1.5×10^{-11} eVm, respectively.

In order to show how the RSOC and the DSOC influence three components of spin polarization when two SOC terms coexist, S_i for fixed DSOC strength are shown in Fig.4 and Fig.5 respectively. From Fig.4 for the in-plane spin polarizations, one can see that when the RSOC strength α_R enhanced, S_x and S_y present more longitudinal oscillations and its precession length decreased accordingly. This result also demonstrates the oscillations for different SOC strength cases are intrinsic, such as in Fig.4(d) and Fig.4(h) $L_{SOC}=\pi\hbar^2/(2m^*\sqrt{\alpha_R^2+\beta_D^2})$=119.7 nm ≈120 nm which can be clearly seen from two figures. In Fig.5 for the out of plane spin polarization with the increase of RSOC strength α_R from 0.5×10^{-11} eVm to 2.5×10^{-11} eVm, S_Z gradually transforms into out of plane spin accumulation, and when α_R is much smaller than β_D no spin accumulation forms. From Fig.5 one can also find that S_Z shows more longitudinal oscillations with the enhancement of α_R indicating the spin accumulation is similarly intrinsic.[20]

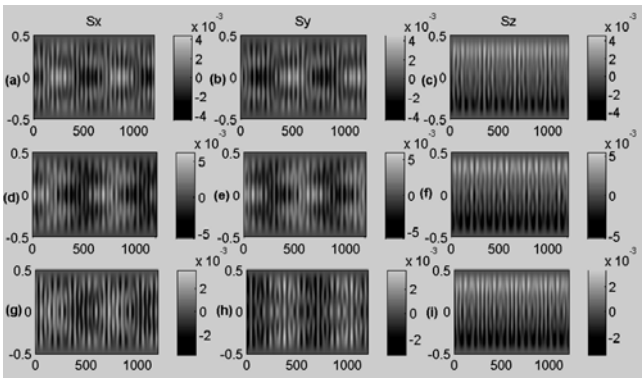

Figure 6. The spin polarization S_i (i=x,y,z) for the case of $\alpha_R=1.0\times10^{-11}$ eVm (a-c), $\alpha_{RN}=\alpha_R=1.0\times10^{-11}$ eVm (d-f) and $\beta_{DN}=\alpha_R=1.0\times10^{-11}$ eVm (g-i). The number of propagation modes n=3 and other SOC terms are taken as 0 respectively.

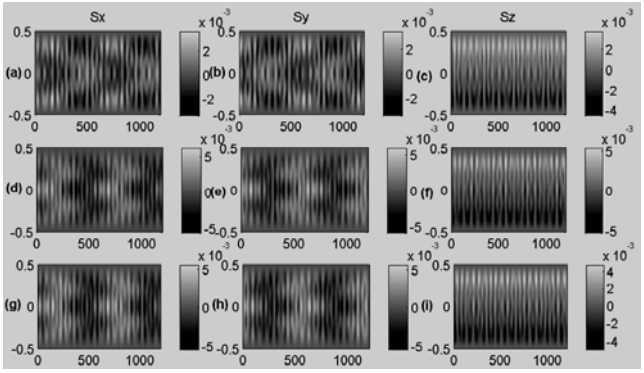

Figure 7. The spin polarization S_i (i=x, y, z) for the case of $\alpha_{RN}=0.5\times10^{-11}$ eVm (a-c), 1.0×10^{-11} eVm (d-f) and 1.5×10^{-11} eVm (g-i) with fixed $\alpha_R=1.0\times10^{-11}$ eVm. The number of propagation modes n=3 and $\beta_D=\beta_{DN}=0$.

In Fig.6 and Fig.7, the influences of SOC in two leads on S_i (i=x, y, z) has been discussed. From Fig.6, one can find that the existence of RSOC or DSOC in two leads does not change the period of longitudinal oscillations, but it shifts the oscillations of in-plane spin polarizations. Moreover, the RSOC in two leads enhances the strength of three components of spin polarization while the DSOC in two leads decreases the strength of three components. From Fig.7, when the RSOC strength α_{RN} for two leads increase, the longitudinal oscillations of in-plane spin polarizations have been shift and the strength of three components have been changed accordingly, indicating that one can modulate the amplitude of spin accumulation by changing the strength of α_{RN}. For the DSOC in two leads case, our calculations obtain the same results. Nonetheless, it is concluded that the existence of two SOC terms in two leads have little influences on spin polarizations.

IV. CONCLUSIONS

In this paper, we have studied spin polarizations of the QW attached by two leads with the coexistence of RSOC and DSOC using scattering matrix approach. It has been found that two inverse direction peaks of the out-of-plane spin polarization S_z shift to two edges of the QW with the increasing propagation modes when only the RSOC appended, while no spin accumulation exists when only the DSOC exists, moreover, when two SOC terms coexist the influences of RSOC are dominant and the out-of-plane spin accumulation still presents while symmetry of the spin accumulation is broken due to the existence of DSOC. Furthermore, the intrinsic oscillations of spin polarizations due to spin precession can be used to identify intrinsic spin accumulation by changing two SOC terms. Finally, when two SOC terms exist in the QW and two leads, the RSOC in two leads enhances the strength of spin polarizations while the DSOC in two leads decrease them, as well as the out-of-plane spin accumulation still present and two SOC terms in the leads shift intrinsic oscillations and change the strength of spin accumulation accordingly, which means that one can also realize the manipulation of spin polarization and spin accumulation using the SOC terms in two leads.

ACKNOWLEDGMENT

This work was financially supported by the Natural Science Foundation of Hunan Province, China (Grant No. 13JJ6097) and the Scientific Research Fund of Hunan Provincial Education Department, China (Grant No. 16A081) .

REFERENCES

[1] P. Fabio, “Spintronics”, Nature Material, vol.11, pp.367, 2012.

[2] T. Dietl, H. Ohno, “Dilute ferromagnetic semiconductors: Physics and spintronic structures”, Review of Modern Physics, vol.86, pp. 187, 2014.

[3] C. Kloeffel and D. Loss, “Prospects for Spin-Based Quantum Computing”, Annu. Rev. Condens. Matter. Phys., vol.4, pp. 51, 2013.

[4] D. A. Pesin, A. H. MacDonald, "Spintronics and pseudospintronics in graphene and topological insulators", Nature Material, vol.11, pp. 409, 2012.

[5] M. Z. Hasan and C. L. Kane, "Colloquium: Topological insulators", Review of Modern Physics, vol.82, pp. 3045, 2010.

[6] M. Konig, S.Wiedmann, C. Bru$ne, A. Roth, H. Buhmann, L.W. Molenkamp, X.-L. Qi, and S.-C. Zhang, "Quantum spin Hall insulator state in HgTe quantum wells", Science, vol.318, pp. 766, 2007.

[7] Y. Kato, R. C. Myers, A. C. Gossard and D. D. Awschalom, "Coherent spin manipulation without magnetic fields in strained semiconductors", Nature, vol.427, pp. 50, 2003.

[8] G. Engels, J. Lange, Th. Schaers and H. Luth, "Experimental and theoretical approach to spin splitting in modulation-doped $In_xGa_{1-x}As/InP$ quantum wells for $B \rightarrow 0$", Physical Review B, vol.55, pp.R1958, 1997; C. M. Hu, J. Nitta, T. Akazaki, H. Takayanagai, J. Osaka, P. Pfeffer and W. Zawadzki, "Zero-field spin splitting in an inverted $In_{0.53}Ga_{0.47}As/In_{0.52}Al_{0.48}As$ heterostructure: Band nonparabolicity influence and the subband dependence, Physical Review B, vol.60, pp.7736, 1999; D. Grundler, "Large Rashba Splitting in InAs Quantum Wells due to Electron Wave Function Penetration into the Barrier Layers", Physical Review Letters, vol.84, pp. 6074, 2000.

[9] G. Dresselhaus, "Spin-Orbit Coupling Effects in Zinc Blende Structures", Physical Reviews, vol.100, pp.580, 1955.

[10] M. I. D'yakonov and V. Yu. Kachorovskii, "Spin relaxation of two-dimensional electrons in noncentrosymmetric semiconductors", Sov. Phys. Semicond., vol.20, pp. 110, 1986.

[11] G. Lommer, F. Malcher and U. Rosler, "Spin splitting in semiconductor heterostructures for $B \rightarrow 0$", Physical Review Letters, vol.60, pp.728, 1988.

[12] S. Prabhakar, R. Melnik and L. L. Bonilla, "Electrical control of phonon-mediated spin relaxation rate in semiconductor quantum dots: Rashba versus Dresselhaus spin-orbit coupling", Physical Review B, vol.87, pp.235202, 2013; T. Meng, J. Klinovaja and D. Loss, "Renormalization of anticrossings in interacting quantum wires with Rashba and Dresselhaus spin-orbit couplings", Physical Review B, vol.89, pp.205133, 2014; A. Dyrdał, J. Barnaś and V. K. Dugaev, "Spin Hall and spin Nernst effects in a two-dimensional electron gas with Rashba spin-orbit interaction: Temperature dependence", Physical Review B, vol. 94, pp.035306, 2016.

[13] J. Schliemann, J. Carlos Egues and D. Loss, "Nonballistic Spin-Field-Effect Transistor", Physical Review Letters, vol.90, pp.146801, 2003.

[14] M. Wang and K. Chang, "Anisotropic spin transport in two-terminal mesoscopic rings: Rashba and Dresselhaus spin-orbit interactions", Physical Review B, vol.77, pp.125330, 2008.

[15] J. L. Cheng, M. W. Wu and I. C. da Cunha Lima, "Anisotropic spin transport in GaAs quantum wells in the presence of competing Dresselhaus and Rashba spin-orbit coupling", Physical Review B, vol.75, pp.205328, 2007.

[16] S. D. Ganichev, V.V. Bel'kov, L. E. Golub, E. L. Ivchenko, Petra Schneider, S. Giglberger, J. Eroms, J. De Boeck, G. Borghs, W.Wegscheider, D.Weiss and W. Prettl, "Experimental Separation of Rashba and Dresselhaus Spin Splittings in Semiconductor Quantum Wells", Physical Review Letters, vol.92, pp.256601, 2004.

[17] S. Giglberger, L. E. Golub, V. V. Bel'kov, S. N. Danilov, D. Schuh, C. Gerl, F. Rohlfing, J. Stahl, W. Wegscheider, D. Weiss, W. Prettl and S. D. Ganichev, "Rashba and Dresselhaus spin splittings in semiconductor quantum wells measured by spin photocurrents", Physical Review B, vol.75, pp.035327, 2007.

[18] M. Scheid, M. Kohda, Y. Kunihashi, K. Richter and J. Nitta, "All-Electrical Detection of the Relative Strength of Rashba and Dresselhaus Spin-Orbit Interaction in Quantum Wires", Physical Review Letters, vol.101, pp.266401, 2008.

[19] J. Yao and Z. Q. Yang, "Spin accumulation in a ballistic Rashba bar", Physical Review B, vol.73, pp.033314, 2006.

[20] J. Wang, K. S. Chan and D. Y. Xing, "Intrinsic oscillation of spin accumulation induced by Rashba spin-orbital interaction", Physical Review B, vol.73, pp.033316, 2006.

[21] S. H. Chen, M. H. Liu, K. W. Chen and C. R. Chang, "Broken spin-Hall accumulation symmetry by magnetic field and coexisted Rashba and Dresselhaus interactions", Journal of Applied Physics, vol.101, pp.09D513, 2007.

[22] S. K. Pandey, "Spin accumulation due to double refraction at lithographic boundaries", arXiv:1404.1453v1, 2014.

[23] A. V. Moroz and C. H. W. Barnes, "Effect of the spin-orbit interaction on the band structure and conductance of quasi-one-dimensional systems", Physical Review B, vol.60, pp.14272, 1999.

[24] F. Kassubek, C. A. Stafford and H. Grabert, "Force, charge, and conductance of an ideal metallic nanowire", Physical Review B, vol.59, pp.7560, 1999.

[25] X. F. Wang, "Spin transport of electrons through quantum wires with a spatially modulated Rashba spin-orbit interaction", Physical Review B, vol.69, pp.035302, 2004.

[26] Q. F. Sun and X. C. Xie, "Spontaneous spin-polarized current in a nonuniform Rashba interaction system", Physical Review B, vol.71, pp.155321, 2005.

[27] M. H. Liu and C. R. Chang, "Nonuniform Rashba-Dresselhaus spin precession along arbitrary paths", Physical Review B, vol.74, pp.195314, 2006.

[28] B. K. Nikolic and S. Souma, "Decoherence of transported spin in multichannel spin-orbit-coupled spintronic devices: Scattering approach to spin-density matrix from the ballistic to the localized regime", Physical Review B, vol.71, pp.195328, 2005.